Part II. Theoretical Analysis of Coalescence Rate

Theoretical models for the drainage of the liquid film between a droplet and the interface have been presented in which the thickness of the film is assumed to vary. The models have been used to derive expressions for the film drainage time and the pressure drop through the film. The experimental results presented in Part I of this paper, when inserted into the equations, show that the drainage film is thinnest at its periphery. These conclusions have been supported by high-speed photography and have been used to explain the distribution of coalescence times reported by all investigators in this field.

Gillespie and Rideal (3) first postulated that coalescence time was the period required for drainage of a film of the upper phase liquid from in between the droplet and the interface. Since that time many idealized models have been proposed to describe the approach of the droplet to the interface and the drainage of the film prior to coalescence. These models are illustrated in Figures 1*a*, *b*, *c*, and *d*.

Charles and Mason (4) considered a rigid curved surface approaching a flat stationary plane under the action of a force F. The space between the surface and the plane contained a liquid of viscosity μ_2, the minimum distance between the surface and the plane at the vertical mid axis was h, and at any radius r from this axis the distance between the plane and the surface was taken to be ξ. ξ was a function of r. By assuming that the velocity of the liquid being squeezed out u was a function r and that the velocity profile was parabolic, Charles and Mason equated the work done by the force F to the energy dissipated by friction to obtain the expression

$$V = -\frac{dh}{dt} = \frac{F}{6\pi\mu_2 \int_o^r \frac{r^3}{\xi^3} dr} \tag{1}$$

The droplet surface was assumed to be parabolic, and therefore

$$\xi = h + r^2/2a \tag{2}$$

which on substitution in Equation (1) and integrating from $r = 0$ to $r = a$ and between the limits h_1 and h_2 gave

$$t_{1,2} = \frac{\mu_2}{2\,\Delta\rho\, ga} \ln \frac{h_1}{h_2} \tag{3}$$

when $a >> h$ and $\Delta\rho$ is the density difference of the phases. When the droplet and the surface were parallel disks $\xi = h$, and the radius of the flattened part of the droplet R_o was given by

$$R_o = a^2 \left[\frac{2\,\Delta\rho\, g}{\gamma^2}\right]^{1/2} \tag{4}$$

where γ was the surface tension of the upper phase. Integration of Equation (1) under these conditions gave

$$t_{1,2} = \frac{\mu_2}{4}\left[\frac{\Delta\rho\, g\, a^5}{\gamma^2}\right]\frac{1}{h_2^2} \tag{5}$$

where $h_1 >> h_2$.

Equations (3) and (5) apply to two-component system only, since the analysis does not consider electric double layer, electroviscous effects, or van der Waal forces. Furthermore the surfaces were assumed rigid, and therefore Chappelear (13) and Lang (6) carried out their analysis on the basis of model (*c*) in Figure 1. They assumed that the film was uniformly thick, and the expression obtained for drainage time was not very different from Equation (3).

Model (*d*) in Figure 1 was proposed by Elton and Picknett (2). The value of R was arbitrarily fixed, and models (*b*) and (*c*) are the limiting cases for $R = \infty$ and and $R = a$. The drainage equation derived for this model differed little from Equation (3). Models (*a*), (*b*), (*c*), and (*d*) in Figure 1 are restricted to small droplets. However Princem (14) derived equations giving the pressure inside the droplet and in the film from which he was able to estimate the excess pressure across the curved surface of the droplet. From this the drop share at the interface was predicted and the area of the film calculated. The drainage equations were then applied to large droplets by assuming that the film was uniformly thick and the drainage time equation obtained was

$$t_{1,2} = \frac{3\,\mu_2\, a^3}{\gamma} \cdot \frac{1}{a_2^3} \tag{6}$$

when $h_1 >> h_2$. Equations (3), (5), and (6) illustrate the conflicting effects of $\Delta\rho$ as was shown experimentally in Part I of this paper. Furthermore if coalescence time is equivalent to drainage time, it is evident that none of the drop approach models agree with the coalescence time results presented, as the drainage time varies from $t \propto a^{-1}$ for the spherical-planar model (2) to $t \propto a^5$ for a film of uniform thickness. Thus it would appear that to satisfy the results reported for the benzene-water system, that $t \propto a$, a mixed model possessing a drainage film of nonuniform thickness is necessary. In addition Chappelear (13) has pointed out that the assumption of a drainage film of uniform thickness disagrees with the fact that the pressure in the thinning film must decrease in

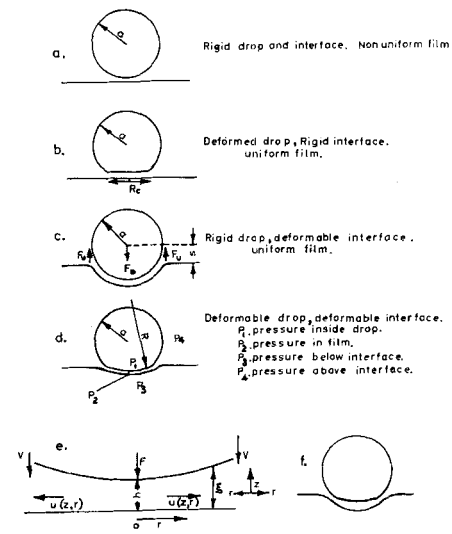

Fig. 1. Idealized models of approach of drop to interface.

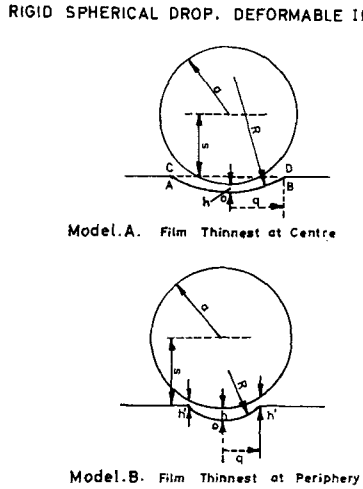

Fig. 2. Proposed coalescence time models.

the direction of flow, with accompanying variations in the film thickness. The minimum thickness of the film may be on the vertical mid axis or at the droplet periphery. Dimpling of gas bubbles at a liquid-gas interface is well known (*15*), (*16*), and a similar geometry has been suggested for liquid droplets (*16*). However Charles and Mason (*4*) did not observe actual dimpling at the interface and proposed a drop profile of the type shown in Figure 1*f*. Therefore it is probable that the thickness of the drainage film varies between the vertical mid axis and periphery, and the following model is submitted to allow for such a variation.

PROPOSED MODEL

The film in between the droplet and interface can vary in thickness through the droplet possessing a dimple in its base, or the cavity in the interface can be of larger radius than the radius of curvature of the base of drop, or the radius of curvature on the droplet can be greater than the radius of the cavity. Charles and Mason (*4*) did not observe dimpling of the droplet surface and therefore the two idealized models shown in Figure 2, in which the droplet is assumed to be spherical and the interface is deformed, is submitted. In model (*A*) the film is thinnest at the center. In model (*B*) the film is thinnest at its periphery. In both diagrams the value of R is arbitrary, and the thickness of the film is exaggerated.

The distance s is obtainable from a force balance when the presence of the film is ignored because $h << a$. The upward force F_u due to surface tension is expressed as

$$F_u = \frac{2\pi(a^2 - s^2)\gamma}{a} \tag{7}$$

and the downward force F_D is equal to the weight of that part of the drop above the interface. That is

$$F_D = \frac{4}{3}\pi a^3 [\rho_1 - \rho_2]\, g - \pi\left[\frac{2}{3}a^3 - a^2 s + \frac{s^3}{3}\right]$$

$$(\rho_1 - \rho_2)g = \pi g\,(\rho_1 - \rho_2)\left(\frac{2}{3}a^3 + a^2 s - \frac{s^3}{3}\right) \tag{8}$$

or

$$s\left[1 + \frac{2s\gamma}{a^3(\rho_1 - \rho_2)g} - \frac{s^2}{3a^2}\right] = \frac{2\gamma}{a(\rho_1 - \rho_2)g} - \frac{2a}{3} \tag{9}$$

In order to apply Equation (1) to the drainage of a film of nonuniform thickness it is necessary to express the film thickness as a function of radius r. Hence consider the following.

MODEL A

Let it be assumed that the profile of the surface of the droplet and the deformed part of the interface can be represented by parabolas having the same radii of curvature at the apex. This is reasonable since s is only slightly smaller than a; that is deformation is small. Close to the origin 0 the equation of the drop profile is

$$Z \doteq h + \frac{r^2}{2a} \tag{10}$$

and that of the interface is

$$Z = \frac{r^2}{2R} \tag{11}$$

For small deformations the vertical depth of the film is approximately equal to the film thickness, so that ξ becomes

$$\xi = h + \left(\frac{1}{2a} - \frac{1}{2R}\right)r^2 = h + \phi r^2 \tag{12}$$

from Equations (10) and (11). In Equation (12) $\phi = \left(\frac{1}{2a} - \frac{1}{2R}\right)$. When $R \to \infty$, Equation (12) is reduced to $[\xi = h + r^2/2a]$ giving the spherical-planar model; when $R \to a$, Equation (12) becomes $[\xi = h]$ giving the uniform thick film model for a rigid drop and a deformed interface.

In order to predict the drainage time by Equation (1) the integral $\left[\int_o^q (r/\xi)^3\, dr\right]$ must be evaluated between o and q in Figure 2*a*. From Figure 2*a*, $q \doteq \sqrt{2R(a-s)}$, and

$$\int_o^q \left(\frac{r}{\xi}\right)^3 dr = \frac{1}{2\phi^2}\left[\frac{h}{2\{h + 2R\,\phi(a-s)\}^2} - \frac{1}{h + 2R\phi(a-s)} + \frac{1}{2h}\right] \tag{13}$$

Substitution of Equation (13) into Equation (1) and integration over the limits h_1 to h_2 gives

$$t_{1,2} = -\frac{6\pi\mu_2}{4F\phi^2}\left[\ln\frac{h_2}{h_1} + \ln\left(\frac{h_1 + \theta}{h_2 + \theta}\right) + \frac{\theta}{h_2 + \theta} - \frac{\theta}{h_1 + \theta}\right] \tag{14}$$

where

$$\theta = 2R\phi(a - s)$$

Let R be a multiple of the drop radius a, say $R = \lambda a$; then

$$\phi = \frac{1}{2a}\left(1 - \frac{1}{\lambda}\right) \quad \text{and} \quad \theta = (\lambda - 1)(a - s) \tag{15}$$

Hence the drainage time for different values of λ can be

Table 1. Relation Between s and a for Water Drops at a Benzene-Water Interface at 20°C.

a, cm.	s, cm.
0.20	0.191
0.25	0.233
0.30	0.269
0.35	0.300

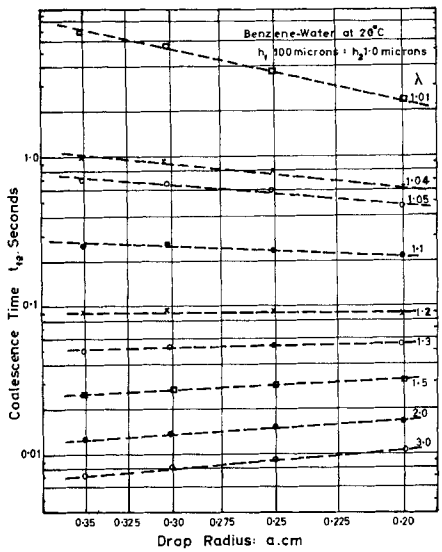

Fig. 3. Variation of calculated drainage times with drop size.

calculated for any physical system by means of Equations (14) and (15).

MODEL B

Derivation of the drainage time equations for model *B* is similar to that given above for model *A*. The final equation is

$$t_{1,2} = -\frac{6\pi\mu_2}{4\phi^2 F}\left[\ln\left(\frac{h'_2-\theta}{h'_1-\theta}\right)+\ln\frac{h'_1}{h'_2}+\frac{\theta}{h'_2}-\frac{\theta}{h'_1}\right] \tag{16}$$

where the terms in Equation (16) have the same significance as in Equation (14). λ is less than unity and the minimum thickness $h' = h + \theta$, where h is the film thickness on the vertical mid axis at $r = 0$.

APPLICATION OF DRAINAGE TIME EQUATIONS

Equations (14) and (16) were applied to the experimental results presented in Part I of this paper.

Values of s were calculated for water drops of different diameters residing on a benzene-water interface at 20°C., and the results of these calculations are presented in Table 1. These results show that over the range of drop sizes studied the interface deformation is small. Arbitrary limits of $h_1 = 100 \times 10^{-4}$ to $h_2 = 1.0 \times 10^{-4}$ cm. were chosen and

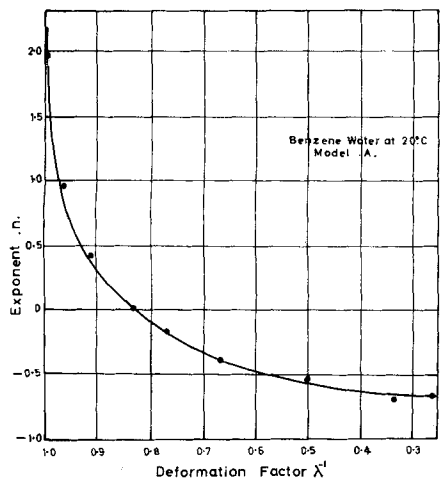

Fig. 4. Variation of n with λ in the relation $-t_{1,2} \propto a^n$.

TABLE 2. EFFECT OF FILM THICKNESS ON DRAINAGE TIMES

h_1	h_2	$t_{1,2}$, sec.
1,000	1.0	0.61
100	1.0	0.608
50	1.0	0.605
10	1.0	0.574
100	0.1	2.158
50	0.1	2.154

the drainage times calculated for different values of λ; the results are presented in Figure 3. The relation between (ln a) and (ln $t_{1,2}$) is slightly curved in each case, but over the range of drop sizes studied straight lines give a good approximation. Hence in the expression $t \propto a^n$, n passes from negative to positive values as λ decreases, as shown in Figure 4 where n is plotted against $1/\lambda$. It is possible that n tends to -1 as $(1/\lambda) \rightarrow 0$, that is as $\lambda \rightarrow \infty$ as for the spherical-planar model. Also as $\lambda \rightarrow 1.0$, n becomes large approaching $n = 5$ as required by the uniform thickness film model.

Equation (14) also shows the effect of the initial thickness of the film on drainage time. This is illustrated in Table 2, where h_1 has been varied between 1,000 and 10 μ with h_2 constant at 1.0 and then at 0.1 μ. In these calculations $\lambda = 1.04$, and the water drop diameter a in benzene is 0.2 cm.

Table 2 shows that in the range of film thicknesses 0.1 to 1.0 μ the drainage time is little affected by h_1 provided the latter is greater than 50 μ. Therefore a value of $h_1 = 100$ μ was arbitrarily selected and the drainage times, for different values of h_2, calculated from Equation (14). The results are plotted in Figure 5. This figure shows the variation of the minimum separation of the drop and interface with time and also confirms that coalescence occurs before drainage is complete. However it is immediately deduced from Table 2 and Figure 5 that coalescence time is greatly affected by the ultimate thickness of the film prior to rupture. Hence application of model *A* to the experimental coalescence time results entails the selection of appropriate values of λ and h_2 in order to obtain a theoretical relationship between the time $t_{1,2}$ and drop diameter a that is similar to the experimental relation between $\bar{t}_{1/2}$ and a. This presupposes that drainage and coalescence times are equivalent, that the time scales of $t_{1,2}$ and $\bar{t}_{1/2}$ are coincident, and that the film thickness at rupture $h_{1/2}$ is constant for drop size. The last supposition

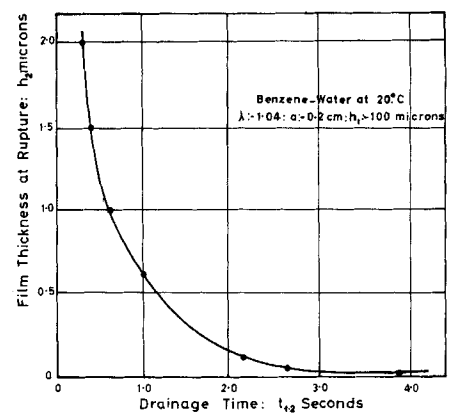

Fig. 5. Effect of film thickness on drainage time.

TABLE 3. RUPTURE THICKNESSES PREDICTED FOR THE BENZENE-WATER SYSTEM BY THEORETICAL MODEL A

Temperature, °C.	$h_2 = h_{1/2}$
20	0.33μ
25	0.33
30	0.36
35	0.38
40	0.42

has been substantiated by Lang (*6*) who stated that drop size did not affect the probability of rupture of the film.

The theoretical model was tested with the experimental benzene-water data. It was found that $\lambda = 1.015$ gave the best approximation to the equation, and the values of h_2 that satisfy Equation (14), when $t_{1,2} = \bar{t}_{1/2}$, are reported in Table 3. These give the thickness of the film at the instant of rupture at different temperatures. In this table it can be seen that the film rupture thickness increases with rise of temperature, which is as would be expected from consideration of the changes in density and viscosity of the film. The values of h_2 in Table 3 were then used to prepare the plots of coalescence time vs. drop size shown in Figure 6. These curves give a fairly good representation of the experimental results, which are also shown on the figure for drops in the size range $a = 0.2$ to 0.3 cm. At 25°C. there is some deviation for the larger drops studied.

A similar analysis to that presented above was carried out on model *B* with Equation (16) used. It was found that the exponent n in $t_{1,2} \propto a^n$ was independent of h'_2 and λ, and n was approximately constant at 2.5. Therefore it was not possible to fit this model to any of the experimental results as the drainage film thickness at rupture was independent of the drop size.

ANALYSES OF PRESSURE DROP IN DRAINAGE FILM

Consider a droplet to approach an interface by squeezing out liquid, of the upper phase, from in between the drop and the interface. The liquid in between the drop and the interface is made to flow and therefore there will be a pressure drop from the vertical mid axis to the periphery of the droplet. The situation will be as represented in Figure 7. Thus consider the element in *ABCD* to be an annulus in the drainage film. Then, the continuity equation of flow through the element is

$$\frac{\delta}{\delta r}\left[r \int_o^\xi u\, dz \right] = r\frac{dh}{dt} \tag{17}$$

where the symbols are as given in Figure 7. Assuming that the velocity profile is parabolic and u is a function of r one gets

$$u = z\,(\xi - z)\,f\,(r) \tag{18}$$

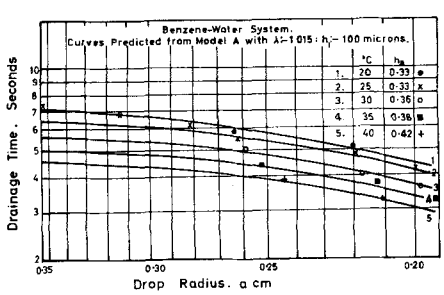

Fig. 6. Comparison of theoretical drainage times.

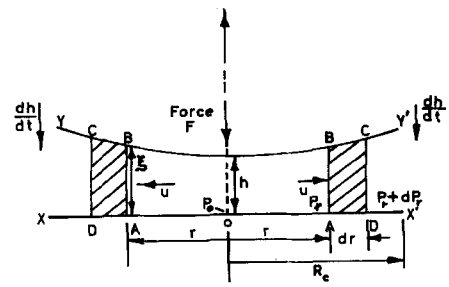

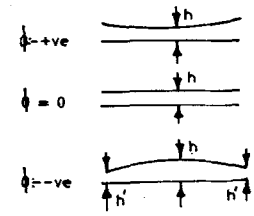

Fig. 7. Film pressure drop models.

and from (16) and (17)

$$f(r) = -\frac{3r}{\xi^3}\left(\frac{dh}{dt}\right) \tag{19}$$

A rate of momentum balance over the element *ABCD* gives

$$-4\pi r\mu_2\left(\frac{\partial u}{\partial z}\right)\Bigg|_{z=0} dr - \frac{\partial}{\delta r}\left[2\pi r\rho_2 \int_o^\xi u^2 dz \right] dr - 2\pi r\xi dP = 0 \tag{20}$$

In Equation (20) it has been assumed that the velocity profile is symmetrical and

$$-\frac{\partial u}{\partial z}\Bigg|_{z=0} = \frac{\partial u}{\partial z}\Bigg|_{z=\xi}$$

From Equations (18) and (19)

$$\frac{\partial u}{\partial z}\Bigg|_{z=0} = -\frac{3r}{\xi^2}\left(\frac{dh}{dr}\right) \tag{21}$$

which on substitution into Equation (20) and integration gives

$$\frac{3}{2}\mu_2\left(\frac{dh}{dt}\right)\frac{r^2(2h+\phi r^2)}{h^2(h+\phi r^2)^2} - \frac{3}{20}\rho_2\left(\frac{dh}{dt}\right)^2\frac{r^2(2h+\phi r^2)}{h(h+\phi r^2)^2} - \frac{3}{20}\rho_2\left(\frac{dh}{dt}\right)^2\frac{r^2}{h(h+\theta r^2)} = P_r - P_0 \tag{22}$$

Finally an energy balance may be made by equating the rate of working of the force F, obtainable from Equations (7) and (8), to the rate of dissipation of energy due to viscous forces. The result is Equation (1) first presented by Charles and Mason (*4*) which may be simplified to

$$\frac{dh}{dt} = -\frac{2F\,h(h+\phi R_c^2)^2}{3\,\mu_2 R_c^4} \tag{23}$$

since $\xi = h + \phi r^2$. Substitution of Equation (22) into (23) gives

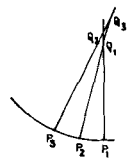

a.

Method of Estimating Radii R_1 and R_2

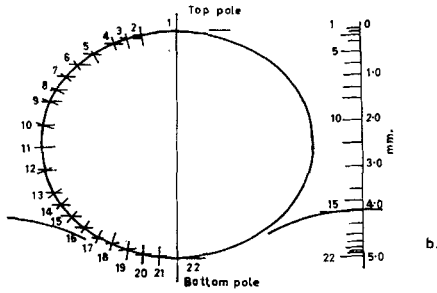

b.

Fig. 8. Profile of water drop at benzene-water interface.

$$-\frac{F}{\pi}\left[\frac{r^2(2h+\phi r^2)(h+\phi R_c^2)^2}{h(h+\phi r^2)R_c^4}\right]-\frac{F^2h^2(h+\phi R_c^2)^4\rho_2}{15\pi^2\mu_2^2R_c^8}\left[\frac{r^2(2h+\phi r^2)+r^2(h+\phi r^2)}{h(h+\phi r^2)^2}\right]=P_r-P_0 \quad (24)$$

where R_c is the radius of the periphery of the film. The pressure P_r at any radial distance r can be calculated from Equation (24) if the pressure at the vertical mid axis P_0 is known. When $r = R_c$, $(P_r - P_0)$ is the total radial pressure drop across the film ΔP_f and is expressed by

$$\Delta P_f = -\frac{F(2h+\phi R_c^2)}{\pi h R_c^2}-\frac{F^2\rho_2}{15\pi^2\mu_2^2}\left[\frac{h(2h+\phi R_c^2)(h+\phi R_c^2)^2+h(h+\phi R_c^2)^3}{R_c^6}\right] \quad (25)$$

For films of uniform thickness $\xi = h$ and $\phi = 0$, and Equation (25) becomes

$$\Delta P_f = -\frac{2F}{\pi R_c^2}-\frac{F^2\rho_2 h^4}{15\pi^2\mu_2^2R_c^6} \quad (26)$$

The second term on the right of Equations (25) and (26) is insignificant when h is small. Therefore for thin films ΔP_f is independent of viscosity and film thickness.

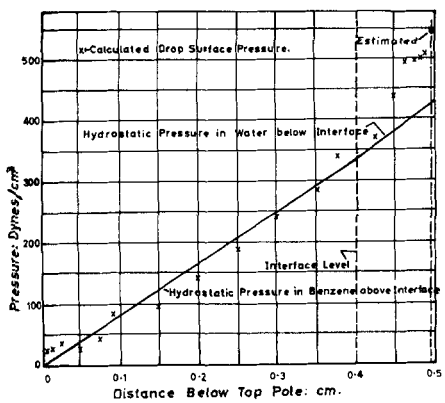

Fig. 9. Calculated surface and hydrostatic pressure outside drop.

In order to evaluate the system completely it is necessary to know the surface pressure of the droplet, and this was done by a method similar to that of Macdonald (17) who studied the shape of raindrops. That is the surface pressures were calculated by measuring the radii of curvature of the drop from photographs of the drop profile. These were inserted into the Laplace equation

$$P_s = \gamma\left(\frac{1}{R_1}+\frac{1}{R_2}\right) \quad (27)$$

where γ is the interfacial tension and R_1 and R_2 are the principal radii of curvature of the droplet. The principal radii of curvature were estimated as follows. The drop profile of a water drop at a benzene-water interface was obtained from a cine photograph by projection on to squared paper, and the profile was as shown in Figure 8*b*. The profile was treated in the manner shown in Figure 8*a*. Thus at the pole point R_1 was assumed to equal R_2 and given by P_1Q_1, where Q_1 was the intersection of the normals to the curve at P_1 and P_2. A third normal was constructed at P_3 to intersect the other normals, as illustrated, to give $R_1 = P_2Q_3$ and $R_2 = P_2Q_1$.

This procedure was repeated around the curve, and R_1 and R_2 was determined at points 1 to 22 on the profile. The excess pressure ΔP_s was calculated for each point from Equation (27). In addition the hydrostatic pressure inside and outside the drop at each point was determined by letting the datum of pressure be zero at point 1. The surface pressure was then calculated from ΔP_s and the hydrostatic pressure inside the drop by assuming that there was no appreciable liquid circulation inside the droplet. The detailed results are presented in reference 9, and the calculated surface pressures P_s are compared with the hydrostatic pressure in the surrounding liquid in Figure 9.

Above the level of the interface there was little variation between P_s and the hydrostatic pressure. The small variations could be errors in the estimation of R_1 and R_2, or they could actually exist indicating some movement of the liquid around the drop surface.

Below the level of the interface the values of P_s were greater than the hydrostatic pressures, and from Figure 9 the pressure in the film was estimated to be 530 dynes/sq.cm. When one considers the pressure drop in the film to be the difference between the surface pressures at points 16 and 22, the maximum estimate of ΔP_f was 154 dynes/sq.cm. This value of ΔP_f was compared with those obtained from Equations (25) and (26) by inserting a value of $R_c = 0.2$ cm. obtained from Equation (25), a value of $a = 0.274$ cm. obtained by assuming that the drop profile in Figure 8*b* was a regular ellipsoid with semimajor and minor axes 0.29 and 0.245 cm., respectively, and the results are shown in Table 4 for selected values of ϕ. If the results in Table 4 are compared with 154 dynes/sq.cm. calculated above, it is seen that ϕ would have to be negative in order that they be of the same magnitude. That is, the film would have to be thinnest at its periphery. This point was further tested by calculating the pressures P_r at different points in the drainage film from Equation (24) with different values of ϕ and com-

Table 4. Pressure Drop in Drainage Film

	$\phi = 0.029$	$\phi = 0$		$\phi = -0.0292$		
h, μ	P_f, dynes/sq. cm.	h	P_f	h	h'	P_f
1.0	1,450	1.0	492	4.5	1.0	296
1.0	592	10.0	492	5.0	0.5	275

paring these values of P_r with values calculated from the drop profile. It was found that the best comparison is obtained for $\phi < 0$.

From the above pressure drop consideration it may be said that the film is of nonuniform thickness and is least thick at its periphery, although the experimental results could not be satisfactorily represented by the drop approach model *B*. Furthermore high speed cine photographs of the coalescence process have shown that frequently coalescence was initiated at the film periphery. Therefore it may be that the type of film profile occurring is not necessarily constant for a given set of conditions, and as the experimental results of $\bar{t}_{1/2}$ used to test the drainage theory were obtained from observations of at least fifty drops, the film profile indicated by the drainage theory might be a mean profile. Changes in the type of profile could result from slight movement of the drop on the interface, which could occur even for a 1.0-cm. distance of fall of the drop. However high-speed photography has shown that coalescence is initiated at the periphery of the film, and it is reasonable to conclude that this corresponds to the thinnest part of the film. This does not justify the postulation of the existence of a dimple in the base of the droplet, but the presence of such an indentation in the drop would bring about settling of the type illustrated in Figure 10, which would explain the distribution of coalescence times reported by all workers in this field. That is, the film drains unevenly with the result that the drop approaches the interface with its major axis inclined and the thinnest part of the film would be concentrated over a smaller area for a greater inclination from the horizontal. Hence a shorter time would be necessary for the rupture thickness to be reached. If a drop settled evenly and the film drained uniformly, the film would be thinnest and equally thin all round its periphery, as shown in Figure 10*c*; coalescence would occur by trapping a droplet of the upper phase liquid in the lower phase. Several instances were observed and photographed of a small drop of the upper phase liquid being thrown down into the bulk of the drop phase liquid on coalescence of a drop at the interface. These small upper phase liquid drops would be formed by even drainage of the film so that rupture occurred simultaneously around the periphery of the film.

CONCLUSIONS

The application of the theoretical models developed has been applied to the experimental results presented in Part I to show that the drainage film between the droplet and the interface is of nonuniform thickness. Also pressure drop calculations in the film have shown that there could be a dimple in the droplet and a cavity in the interface. The distortion of the drop profile is thought to result in an inclination of the droplets approaching the interface which explains the distribution of coalescence time results obtained by all investigators. These findings are supported by high-speed photography.

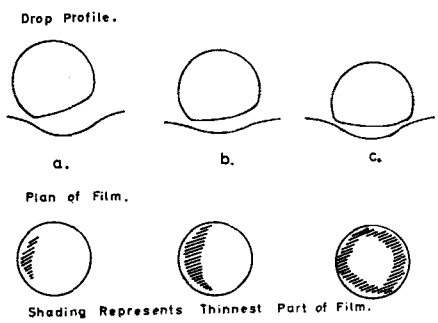

Fig. 10. Possible modes of drop settling and draining.

ACKNOWLEDGMENT

The authors wish to thank the late Professor F. H. Garner of the Chemical Engineering Department of the University of Birmingham, England, for his help and advice throughout this investigation.

NOTATION

a = radius of droplet
A = area of drainage film, statistical drop size factor
c = coefficient in coalescence time distribution equation
F = force, statistical interfacial tension factor
g = acceleration due to gravity
h = drainage film thickness
K = constant in Gillespie-Rideal equation
K_2 = constant in coalescence time correlation
L = distance of fall of drop to interface, statistical descent factor
n = exponent in coalescence time equation
n_1 = exponent in coalescence distribution equations
n_2 = exponent in Gillespie-Rideal equation
N = number of drops coalescing in time t
N_o = total number of drops considered
P = pressure in drainage film
q = composite limit equal to $2R(a - 5)$
r = radius to a point in drainage film
R = film radius
s = depth of interface cavity
t = time
T = temperature, statistical temperature factor
$\bar{t}_{1/2}$ = first step half life coalescence time
$t_{1/2}$ = overall half life coalescence time
$\bar{t}_m$ = mean first step coalescence time
t_m = mean overall coalescence time
u = linear velocity of film
V = velocity of approach of droplet to interface, statistical viscosity factor
x_1 = exponent in coalescence time correlation = -2
x_2 = exponent in coalescence time correlation = 0.5
x_3 = exponent in coalescence time correlation = $0.71\ V^{0.5}$
x_4 = exponent in coalescence time correlation = $-0.02\ (F^2/V^{0.5})$
x_5 = exponent in coalescence time correlation = $0.0001\ (F^2/V^{0.5})$
z = coordinate in pressure drop model

Greek Letters

α = amplitude of ripple on interface
γ = surface tension, interfacial tension
μ = viscosity
ξ = perpendicular film thickness at radius r
π = dimensionless group
ρ = liquid density
ϕ = composite parameter $\left(1 - \frac{1}{\lambda}\right) \Big/ 2a$

Subscripts

c = periphery of film
D = downward
f = film, uniform film thickness
r = radial distance
s = drop surface

Numerals

0 = mid axis origin
1 = initial condition or upper phase
2 = final condition or lower phase
½ = experimental

LITERATURE CITED

1. Cockbain, E. G., and T. S. McRoberts, *J. Colloid Sci.*, **8**, 440 (1953).
2. Elton, G. A. H., and R. G. Picknett, "Proceedings Second International Congress, Surface Activity," Vol. 1, p. 288 (1957).
3. Gillispie, T., and E. K. Rideal, *Trans. Faraday Soc.*, **52**, 173 (1956).
4. Charles, G. E., and S. G. Mason, *J. Colloid Sci.*, **15**, 105 (1960).
5. Mackay, G. D. M., and S. G. Mason, *Nature*, **191**, 488 (1961).
6. Lang, S. B., Ph.D. thesis, University of California, Berkeley, California (1962).
7. Jeffreys, G. V., and J. L. Hawksley, *J. Appl. Chem.*, **12**, 329 (1962).
8. Brownlee, K. A., "Industrial Experimentation," 4 ed., H.M.S.O., London, England (1957).
9. Hawksley, J. L., Ph.D. thesis, University of Birmingham, England (1963).
10. Jenson, V. G., and G. V. Jeffreys, "Mathematical Methods in Chemical Engineering," Academic Press, New York (1963).
11. Konnicke, H. G., *Z. Physik Chem. (Leipzig)*, **211**, 208 (1959).
12. Nielsen, L. E., R. Wall and G. Adam, *J. Colloid Sci.*, **13**, 441 (1958).
13. Chappelear, D. C., *ibid.*, **16**, 196 (1961).
14. Princem, H. M., *ibid.*, **18**, 178 (1963).
15. Derjagisin, B. V., and M. Kusakov, *Acta Physicochim*, **10**, 25 (1959).
16. Allan, R. S., G. E. Charles, and S. G. Mason, *J. Colloid Sci.*, **16**, 160 (1961).
17. Macdonald, J. E., *J. Meteorology*, **11**, 478 (1954).

Manuscript received February 24, 1964; revision received August 24, 1964; paper accepted September 9, 1964. Paper presented at A.I.Ch.E. Pittsburgh meeting.

The Mixed Suspension, Mixed Product Removal Crystallizer as a Concept in Crystallizer Design

ALAN D. RANDOLPH

American Potash & Chemical Corporation, Trona, California

Simultaneous population and mass balances have been solved together with a generalized form of nucleation-growth rate kinetics to obtain the form of crystal size distribution (CSD) for several idealized modes of crystallizer operation, including seed crystal removal, product classification, arbitrary solids concentration, and staged vessels. The effect of holding time and feed supersaturation on crystal size in a mixed suspension, mixed product removal (MSMPR) crystallizer was also studied. A representative CSD from an MSMPR crystallizer plus the relative kinetic order of nucleation to growth rate can be used to predict CSD from any of the above modes of operation.

Crystal size distribution (CSD) is one of the most important and troublesome properties of an operating crystallizer and is a property which cannot presently be designed without prior experience with the crystal system and the type of crystallizer used. Saeman (*1*), in a classical contribution to crystallization theory, published equations for the form of steady state size distributions in mixed crystal suspensions. These equations had been derived as early as 1931 by Peet (*2*) in an unpublished report and by Bransom et al. (*3*) in 1948. However, the chief importance of Saeman's work was the presentation of these equations in an engineering context and the evolution of a philosophy (*4*) which regards crystallization as "a crystal suspension on which is maintained certain constraints." Robinson and Roberts (*5*) published a study of residence time distributions, and hence CSD, for a series of perfectly mixed tanks. These equations reduce to those of Saeman for one tank. Randolph and Larson (*6*) used the concept of conservation of population to derive a general equation relating crystal population density to crystal size in a transient system. Transient CSD for various upsets was studied with a model for a single tank mixed suspension crystallizer and assumed nucleation-growth kinetics used. The problem of steady state CSD from staged tanks was also studied, but in this case nucleation in each tank was accounted for. It should be pointed out that in all of the above references only the form or dimensionless behavior of the distribution was predicted; kinetic growth and nucleation rates are necessary to obtain actual CSD for a particular system.

A notable addition to the recent literature is a paper by Bennett (*7*) which tabulates experimental CSD data from a large class of crystallizers and crystal systems. A property of any CSD is the so-called *coefficient of variation* (C.V.),* or *relative size spread* over which the majority

Alan D. Randolph is with the University of Florida, Gainesville, Florida.

* Not to be confused with coefficient of velocity, also referred to as C.V.